MEDIUM PRF SCHEDULES FOR AIRBORNE FIRE CONTROL RADAR

C.M. Alabaster[*], E.J. Hughes[*], S.M. Parry[†], D.A. Wiley[†], J.H. Matthew[#] & P.G. Davies[**]

* Cranfield University, Shrivenham, Nr. Swindon, WILTS. SN6 8LA UK
c.m.alabaster@cranfield.ac.uk Fax: 01793 785902
† Royal Australian Air Force, Australia
# Royal Air Force, UK
** Royal Electrical & Mechanical Engineers, UK

Keywords: Medium PRF Radar, Evolutionary Algorithms, PRF Selection, Decoding, Ghost Targets.

Abstract

Previous work has shown how evolutionary algorithms are an effective tool in optimising the selection of radar pulse repetition frequency (PRF) values for medium PRF schedules. In this paper we review the factors influencing PRF choice and describe the optimisation process, which is driven by the requirement to minimise range/Doppler blindness whilst maintaining full decodability for an airborne fire control radar application. A number of near optimum schedule types are identified; some requiring target data in three PRFs and others in just two. The paper includes detailed justification and ghosting performance analysis to show that in many situations, the schedules requiring data in just two PRFs are a practical alternative to conventional schedules requiring data in three PRFs.

1 Introduction

Airborne fire control systems are required to measure both range and velocity of targets in the presence of very high clutter returns from the ground. Unfortunately, the clutter is spread widely in velocity and also exists in most range cells. Furthermore, the maximum range and required Doppler bandwidth are so large that it is not possible to measure both range and velocity unambiguously with a single waveform. Medium pulse repetition frequency (PRF) waveforms offer the best compromise in all aspect detection performance in the presence of clutter and so have become an attractive mode of operation in many of today's military radar systems. The high level of performance demanded from such systems is dependent on the clutter scenario and on the precise values of PRFs chosen, amongst many other factors. A medium PRF is characterised as being range and velocity ambiguous. Unambiguous range and velocity may be decoded through a comparison of the ambiguous target data received in a minimum number, *M*, PRFs. Each medium PRF is also characterised by having blind ranges associated with eclipsing losses and overwhelming side lobe clutter (SLC) and blind velocities associated with the rejection of main beam clutter (MBC) and its repetition in the frequency domain. The regions of blindness require that a radar must alternate its operation over several, *N*, coherent bursts of PRFs in order to recover sufficient data in the requisite *M* to resolve the ambiguities, in what is known as an *M of N* schedule. A potential problem associated with medium PRF operation is the indication of false targets, known as 'ghosts', resulting from the correlation of the ambiguous returns of one target with those of another or with noise generated false alarms. This is also a function of the schedule type (*M of N*) and precise PRF values but tends to worsen as the number of targets and false alarms increases.

This paper builds on previous work by the authors, [1] and [2] regarding the optimisation of the selection of precise values of PRF for an airborne fire control radar (FCR) using Evolutionary Algorithms (EA). Section two details the factors affecting the choice of PRF and the design of schedules including shorter schedules ($N < 8$) that require target data in only two ($M = 2$) PRFs. The ability to generate fully decodable *2 of N* schedules has led to comparisons between *2 of N* schedules with the more traditional *3 of N* schedules using a model of an airborne FCR to assess the blind zone performances of each and is described in section three. On the whole, the comparisons favour the *2 of N* schedules. However, one of the concerns that *2 of N* schedules raises is the greater likelihood of ghost targets, especially as the number of false alarms in any beam position increases. The likelihood of increased ghosts has therefore led to the formulation of a strategy for decoding true range and velocity whilst minimising the incidence of ghost targets (section four). The results of the blind zone optimisation and the decodability robustness and ghosting performance of a variety of near-optimum schedules are presented in section five. Finally, section six draws some conclusions.

2 Medium PRF Operation

The PRFs of a medium PRF schedule must be selected subject to the following constraints:

- Decodability. All combinations of *M* from *N* must allow true range and Doppler to be decoded. Two of the most popular methods of decoding true range and Doppler are the Chinese Remainder Theorem (CRT) and the Coincidence Algorithm (CA). The CA is preferred here as it is less constraining on PRF choice since it requires only that (1) and

(2) be satisfied for all combinations of *M* PRFs from the total *N*, where LCM is the lowest common multiple, R_{max} is the maximum range and D_{max} is the maximum Doppler bandwidth.

$$LCM\left(PRI_1, \quad PRI_2, \quad .... \quad PRI_M\right) \geq \frac{2R_{\max}}{c} \qquad (1)$$

$$LCM\left(PRF_1, \quad PRF_2, \quad .... \quad PRF_M\right) \geq D_{\max} \qquad (2)$$

- Blindness. The blind ranges and velocities of individual PRFs must be sufficiently dispersed so as to maintain target visibility over the range/Doppler detection space of the radar in as many PRFs as possible.
- Blind Velocities. Blindness over all ranges at particular velocities due to the alignment of the MBC rejection notches (and multiples thereof) in too many PRFs must not be allowed to exist.
- Ghosting. The likelihood of ambiguous returns from one target correlating with those of another target or with a noise generated false alarm should be minimised.
- Maximum PRF. The upper limit is usually governed by the maximum transmitter duty cycle allowable and also through considerations of the repetition of SLC in the time domain. Also, when combined with the FFT size, the maximum frequency bin width may be limited by the required velocity resolution.
- Minimum PRF. The lower limit is governed by the consideration that the MBC rejection should not exceed more than 50% of the Doppler band in order to maintain adequate target visibility.
- Mean PRF. The mean value of the *N* PRFs must be constrained so as to permit the transmission of the entire schedule within the beam dwell time on target.
- FFT size, or alternatively filter bank size and bin width.

The minimum number of PRFs in which target data is required in order to resolve range and Doppler ambiguities is, strictly, two. *2 of N* schedules require PRFs for which every combination of 2 from *N* satisfy (1) and (2). A very fine PRI resolution results in a large number of PRIs/PRFs between the maximum and minimum limits and makes the decodability requirements of (1) and (2) easier to satisfy. Relatively coarse PRI resolution of one range cell, which is typical of many current systems, may prevent *2 of N* schedules satisfying (1) and (2) and so data is required in a third PRF. This study assumes PRI resolution of 10ns and so *2 of N* schedules are viable. An initial study to optimise the selection of *2 of N* schedules has been conducted [3]. This work concluded that if data is required in only two PRFs, as opposed to three, the total number of PRFs in the schedule that is required, *N*, may be reduced. Furthermore, range/Doppler blindness is reduced since the radar is now considered blind in regions where there is visibility in fewer than two PRFs (as opposed to three) or detection may be considered marginal when there is visibility in exactly two PRFs. A shorter overall schedule (reduced *N*) relaxes the constraint on the mean PRI or, alternatively, permits a faster scan rate.

The one danger associated with *2 of N* schedules is the greater likelihood of ghost targets, especially as the number of false alarms increases. *2 of N* schedules will report more self-ghosting targets (the correlation of the ambiguous return of one target with that of another target) and noise ghosts (the correlation of the ambiguous return of one target with a noise generated false alarm) since coincident threshold crossings are required in only two PRFs (as opposed to three). Any target detection appears as a lattice of detection points in range/Doppler detection space due to its repetition in the time and Doppler domains. For a target observed in several PRFs one would observe several such lattices, one for each PRF, with the spacing between points in the time and Doppler domains differing depending on the PRI/PRF. The lattices coincide at the true target range/Doppler, as illustrated in Figure 1, and therefore the regions of lattice coincidence are the basis for decoding the ambiguities.

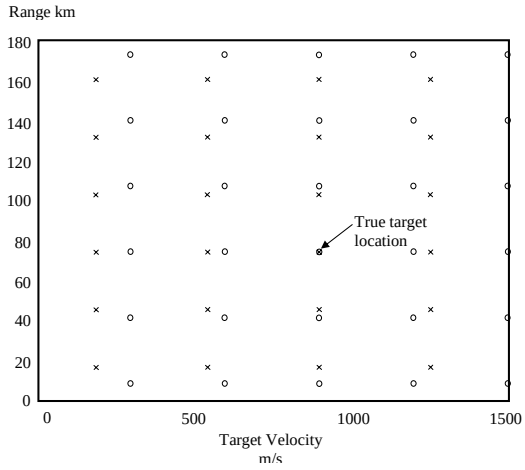

Figure 1: Lattices of Detection Points for One Target Observed in 2 PRFs
x = *target detections in PRF1,* **o** = *target detections in PRF2*

Measurement error corrupts the range/Doppler coordinates of the lattice points, whilst target smear extends the coordinates over a range of values. In this way it is possible that the detection points at the true target coordinates do not coincide precisely but are merely closely grouped *clusters* of up to *N* detection points. It also becomes possible that other clusters coalesce in other regions of the range/Doppler detection space and resolving the ambiguities is no longer possible. These clusters correspond to ghost targets and typically contain fewer detection points than those of genuine targets. Their presence illustrates the problem that the decodability of the schedule is not sufficiently robust to range/Doppler tolerances. The robustness of the decodability of a schedule has been depicted using skyline diagrams in the past [4]. In generating the PRF schedules used in this work a margin for decodability is allowed. No multiples of any two (three) PRIs are allowed to align to within 0.7μs of each other for *2 (3) of N* schedules. In this study, the range cell width = compressed pulse width = 0.5μs; the extra 0.2μs being the decodability margin. If this margin is increased, it becomes less simple for the EA to find allowable PRF schedules and the blind zone performance of the solutions it does find is degraded.

When the lattice points of several targets are displayed on the range/Doppler detection space there becomes a greater likelihood of obtaining false clusters (ghosts), as the number of targets increases. Ironically, the improved blind zone performance of *2 of N* schedules compounds the problem slightly, since more detection points will be visible. Therefore, as *M* is reduced, both the probability of detection and the probability of false alarms increase. The aim is to identify genuine clusters within limits of range/Doppler space and discount the false ones.

3 Optimisation For Minimal Blindness

Figure 2 illustrates the optimisation process that has been employed in the selection of PRFs. The optimisation process is driven by an evolutionary algorithm with an optimisation goal of achieving minimal range/Doppler blindness.

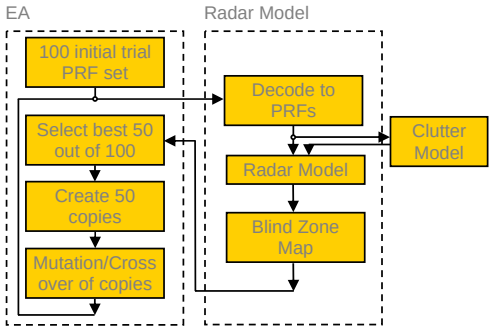

Figure 2: The Optimisation Process

The evolutionary algorithm maintains a population of trial PRF schedules whose values are refined on each iteration of the loop process (generation) along the lines of Darwinian theories of evolution and survival of the fittest [5]. Each trial set is passed to the radar model and the genetic description is decoded to PRF values. This decoding stage employs a variety of checks to ensure that the schedule is decodable, enforces the decodability margin, does not incur any blind velocities and is within the limits of maximum, minimum and mean PRF, as dictated by the radar model. The PRFs are passed to the radar and clutter models. The clutter model returns the clutter map for each PRF which is also passed to the radar model. The radar model is based on an airborne FCR and accepts the trial PRF schedule and clutter maps. The model then generates a blind zone map and quantifies the area of the range/Doppler detection space which is visible in fewer than *M*+1 PRFs. The map represents the area which is blind to the radar (visibility in fewer than *M* PRFs) or where detection is marginal (visible in exactly *M* PRFs) and is used as a measure of the quality of the trial schedule. This metric is passed back to the evolutionary algorithm as the objective value of the trial solution.

The evolutionary algorithm applies rules of cross-over and mutation to produce the next generation of trial solutions. These rules favour the retention of good solutions from previous generations but also allow the exploration of the entire search space. Evolutionary algorithms are powerful optimisation techniques which have been successfully employed in a variety of combinatorial problems. They are particularly adept at finding near-optimum solutions very quickly when the number of possible combinations precludes an exhaustive search. In section five we present results of the evolutionary algorithm optimising the selection of *3 of 8, 2 of 8, 2 of 7, 2 of 6* and *2 of 5* type schedules.

A radar model based on an airborne fire control radar (FCR) type was derived to trial the fitness of PRF sets, details of which are summarised in Table 1.

Parameters	Value
Carrier frequency	10 GHz
Max & Min PRI	150 to 35 µs
PRI resolution	10ns (11501 PRIs)
Transmitted pulse width	7 µs
Compressed pulse width	0.5 µs
FFT size	64 point
PRF changeover time	1.7 ms
Blind range due to eclipsing	15 range cells
Duty cycle	Variable (0.2 peak)
Beamwidth	3.9^0
Scan rate	60^0/s
Target illumination time	65 ms
MBC/GMT rejection bandwidth	± 1.67 kHz (25m/s)
Maximum target Doppler	± 100 kHz (1500m/s)
Maximum detection range	185.2 km (100 nmi)
Target radar cross-section	5 m^2

Table 1: Radar Model Parameters

It is assumed that the radar is flown at an altitude of 5000 metres over a surface with a backscatter coefficient of $0.01m^2/m^2$. The antenna has a beamwidth of 3.9^0 and a constant sidelobe level of -30dB below the main beam. It is further assumed to be directed along a 6^0 depression angle and that platform motion compensation (PMC) is applied to offset the Doppler of the platform velocity resolved along the antenna boresight to zero Hz. The clutter model returns a clutter map calculated for each PRF within all trial schedules. A radar target of $5m^2$ is assumed and any point in the range/Doppler detection space having a signal to clutter ratio (SCR) < 1 is considered blind.

4 Ghosting Performance

The work to optimise the selection of schedules for minimal blindness identified the following near-optimum schedules:

Best *2 of 6*: PRIs (µs)= 64.04, 74.53, 83.03, 92.07, 100.75, 118.80
Best *2 of 7*: PRIs (µs) = 73.55, 81.03, 89.76, 99.42, 109.50, 116.46, 125.17
Best *2 of 8*: PRIs (µs) = 78.92, 81.56, 86.66, 90.46, 99.81, 111.81, 117.09, 128.56
Best *3 of 8*: PRIs (µs) = 63.11, 69.97, 77.07, 81.31, 90.06, 99.90, 109.75, 119.00

Each of the above schedules has been trialled with the input of multiple targets and an algorithm developed to recognise genuine clusters of detections from false ones (ghost targets). Two types of multiple target scenarios have been used; the first places between one and five targets at random values of range and Doppler and the second places 4, 6, 8 or 10 targets at 150m range intervals each with the same Doppler. The former gives a random placement of targets, which is perhaps an unlikely situation in reality whereas the latter represents a close formation, whose range/Doppler centroid is randomly placed on each trial, and is a more likely occurrence. Zero, one or two noise generated false alarms of random range/Doppler may also be added. A small random variation on target range/Doppler is also imparted over successive PRFs to represent random measurement error and has the effect of spreading the clusters slightly.

The algorithm considers the *base targets* initially, i.e. target detection points within the first unambiguous range and Doppler intervals, and repeats these detection points into the lattices of Figure 1 by the addition of multiples of the PRI in range and multiples of the PRF in Doppler. Clusters are then formed through the proximity of detection points in different PRFs. The algorithm is based on the concept that genuine targets are characterised by clusters having a large number of detection points i.e. visible in a large number of PRFs, in a small region of range/Doppler space, whereas ghost targets are more likely to be observed in a few PRFs. It also discounts any clusters containing detection points already attributed to the clusters considered genuine. Therefore, potential ghost target clusters containing the detections of genuine targets which are repeated in the time and frequency domains are dismissed. The proximity of detection points which form clusters is an important variable in the success of the algorithm. Rectangles in range/Doppler space of the following dimensions have been trialled: 80Hz x 0.6µs, 50Hz x 0.6µs, 40Hz x 0.3µs and 25Hz x 0.3µs. These rectangles define the dimensions of the maximum allowable cluster sizes.

Test matrices were derived which explore the various combinations of variables and result in 240 combinations for randomly distributed targets and 192 combinations for close formation targets. Five hundred experiments of each combination were ran in order to generate statistics on the correctly reported targets, additional targets (i.e. ghosts), genuine targets not reported and blind targets.

5 Results & Discussion

5.1 Blindness

One hundred runs of the optimisation process have been conducted and used to generate the statistics of Table 2. The blindness statistics quoted in Table 2 refer to the percentage of the range/Doppler detection space in which targets are visible in fewer than M+1 PRFs and include blindness due to overwhelming SLC, the first blind range and the first blind velocity. Table 2 ranks the schedules in order of blindness performance. Of particular note is the fact that *2 of 6* schedules marginally outperform *3 of 8* schedules.

M from N	Min %	Max %	Mean %	σ %
2 from 5	66.10	66.73	66.43	0.1434
3 from 8	58.37	59.91	59.01	0.2803
2 from 6	56.35	57.70	57.12	0.3316
3 from 9	53.74	55.02	54.46	0.2656
2 from 7	48.90	50.24	49.46	0.3437
2 from 8	44.13	45.21	44.59	0.2296

Table 2: Blindness Results

The blind zone map of the best *2 of 8* schedule is plotted in Figure 3. This has blindness (visibility in fewer than 3 PRFs) extending over 44.13% of the map, the majority of which is due to overwhelming SLC.

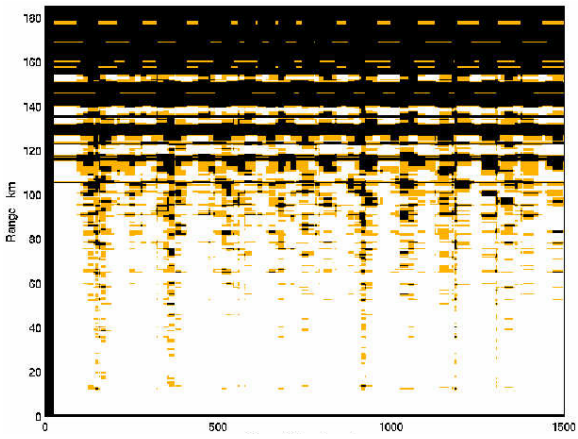

Figure 3: Blind Zone Map of Best *2 of 8* Schedule
(Black = visibility in fewer than 2 PRFs, Grey = visibility in exactly 2 PRFs, White = visibility in more than 2 PRFs)

5.2 Ghosting

Each schedule is quantified in terms of the correctly reported targets, additional (ghost) targets, targets which remained blind and targets not reported (but not blind). All statistics are quoted as percentages of the total number of targets. Thus 500 runs of 4 targets give a total of 2000 targets and 20 occurrences of ghosts would therefore be expressed as 1%.

When one to five random targets were applied approximately 95% of them were correctly reported, irrespective of the schedule, number of false alarms or of the allowable cluster size. The *2 of 8* schedule was consistently the best and the *2 of 6* and *3 of 8* schedules were worst being about 2% lower. Additional ghost targets were generally lower than 0.5% of total applied targets. For ghosting, the *3 of 8* schedule was consistently the best reporting no additional targets in all the runs without false alarms, and only the occasional ghost was seen with 2 false alarms; there was no consistently worst schedule. There was no significant increase in ghosts when one false alarm was applied, however, an increase in ghosts to

around 1 - 4% (depending on allowable cluster size) for the *2 of N* schedules was seen when 2 false alarms and only one or two targets were applied and was attributable to the correlation of one false alarm with the other. Generally, ghost target percentages increased with increasing allowable cluster size but reduced with increasing number of real targets. This is perhaps surprising but is due to the fact that in identifying several genuine targets, the algorithm tags most of the detection points and in so doing the smaller clusters typical of ghosts are more readily discounted. About 5% of applied targets remained blind, irrespective of the numbers of false alarms and allowable cluster size. The blindness statistics of each schedule mirrored their blind zone performances; *2 of 8* being best and *3 of 8* being some 2% higher. Generally, fewer than 1% of targets were not reported, the *3 of 8* schedules being the best.

When 4, 6, 8 or 10 targets in a close formation were applied about 95% were correctly reported and was independent of allowable cluster size and numbers of false alarms but reduced with increasing numbers of targets. The *2 of 8* schedule was consistently best and the *2 of 6* worst being about 5% lower. The reduction with increasing target numbers is due to the greater likelihood of ghosts being reported in preference to genuine targets in regions of marginal visibility. The number of ghosts is somewhat greater for the close formation targets than those of random placement. This is due to the fact that all targets have the same Doppler and so alignment in range only is required to form a ghost. The *2 of 6* schedule reports the highest incidence of ghosts which rises from 1 to 6% as the number of targets increases from 4 to 10. The number of ghosts also rises as the allowable cluster size increases and rises very slightly as the number of false alarms increases. It peaks at a value of around 7.5% for the *2 of 6* schedule (2 false alarms, 10 targets and an allowable cluster size of 80Hz x 0.6μs). The *3 of 8* schedule consistently had the best ghosting performance with a peak value of 1% under similar conditions. Longer schedules tend to result in fewer ghosts as they appear to give rise to clusters having a greater number of detection points which are more readily identified as targets in preference to the smaller clusters of ghosts. The numbers of targets not reported follows the trend in ghosting performance since the reporting of a ghost is usually done in preference to the reporting of a target. Blind target results follow the same pattern as for the random targets which mirror the blind zone performance of each schedule.

It is interesting to note that although *2 of N* schedules do result in more ghost clusters than *3 of N* schedules, the rules of the target extraction algorithm have succeeded in dismissing the vast majority.

6 Conclusions

The evolutionary algorithm has been successful in optimising the selection of PRF values of various medium PRF schedules for minimal range/Doppler blindness. Repeated runs of the EA identify several near optimal PRF sets whose blindness differ marginally from each other. These repeats indicate the existence of several similar local optima in the problem space and the ability of the EA to find them. Blindness is minimised in schedules requiring target data in fewer PRFs ($M = 2$) and for longer schedules ($N = 8$). Of the two, the reduction in M is the most significant. Thus the schedule having least blindness is the *2 of 8* which has some 14% less blindness than the *3 of 8* schedule, and an overall higher probability of detection. The most noticeable improvement occurs at ranges around 60 to 150km, beyond which high sidelobe clutter levels form the dominant cause of blindness.

The numbers of ghost targets remained very low for the *3 of 8* schedules and were only slightly degraded in the *2 of N* schedules. The target extraction algorithm was most reliable for the longer schedules. Close formation targets gave rise to more ghosts than did the targets of random range and Doppler since close formations of identical Doppler only require correlation in range to register as ghosts. Unreported targets were very low in all schedules but tended to follow the trends in the reporting of ghosts. Correctly reported targets were maintained at a high level but were marginally superior for the *2 of 8* schedule. The highest incidence of ghosts (*2 of 6*, close formation targets) also corresponded to the lowest incidence of correctly reported targets, since ghosts were being declared in preference to correct targets. The numbers of blind targets followed the trend in blind zone performance.

In summary, each schedule type has areas of relative strength and weakness, however, the best and worst schedules do not differ appreciably from each other. The original fears regarding the ghosting performance of *2 of N* schedules appear to have been unfounded for the proposed target extraction algorithm. This study has shown that *2 of N* schedules can be considered viable and even advantageous with respect to the more conventional *3 of N* schedules. In particular, the detection performance of an optimal *2 of 6* schedule is very similar to that of an optimal *3 of 8* schedule but enjoys the benefits of being a shorter schedule.

References

[1]. Clive M. Alabaster, Evan J. Hughes and John H. Matthew, “Medium PRF radar PRF selection using evolutionary algorithms”, *IEEE Trans. Aerospace and Electronic Sys*, 39, 3, pp. 990 – 1001, (2003).

[2]. P. G. Davies and E. J. Hughes, “Medium PRF set selection using evolutionary algorithms”, *IEEE Trans. Aerospace and Electronic Sys*, 38, 3, pp. 933-939, (2002).

[3]. Evan J. Hughes and Clive M. Alabaster, “Novel PRF Schedules for Medium PRF Radar”, *Proc. Radar 2003 Conf*, Adelaide, S. Australia, pp. 678 – 683, (2003).

[4]. M. Kinghorn and N. K. Williams, “The decodability of multiple-PRF radar waveforms”, *Proc. IEE Radar 97*, Conf. Publ. No. 449, Edinburgh, UK, pp. 544 – 547, (1997).

[5]. M. S. Zalzala and P. J. Flemming, Eds., *Genetic algorithms in engineering systems*, The IEE, (1997).